ELSEVIER

NeuroImage

www.elsevier.com/locate/ynimg
NeuroImage 21 (2004) 1275–1288

Multimodal assessment of cortical activation during apple peeling by NIRS and fMRI

Masako Okamoto,[a,1] Haruka Dan,[a,1] Koji Shimizu,[b] Kazuhiro Takeo,[b] Takashi Amita,[b] Ichiro Oda,[c] Ikuo Konishi,[c] Kuniko Sakamoto,[a] Seiichiro Isobe,[a] Tateo Suzuki,[a] Kaoru Kohyama,[a] and Ippeita Dan[a,*]

[a] *National Food Research Institute, Tsukuba, Ibaraki 305-8642, Japan*
[b] *Medical Systems Division, Shimadzu Corporation, Nakagyo, Kyoto 604-8511, Japan*
[c] *Technology Research Laboratory, Shimadzu Corporation, Seika-cho, Kyoto 619-0237, Japan*

Received 27 May 2003; revised 25 November 2003; accepted 1 December 2003

An intriguing application of neuroimaging is directly measuring actual human brain activities during daily living. To this end, we investigated cortical activation patterns during apple peeling. We first conducted a pilot study to assess the activation pattern of the whole lateral cortical surface during apple peeling by multichannel near-infrared spectroscopy (NIRS) and detected substantial activation in the prefrontal region in addition to expected activations extending over the motor, premotor and supplementary motor areas. We next examined cortical activation during mock apple peeling by simultaneous measurement using multichannel NIRS and functional magnetic resonance imaging (fMRI) in four subjects. We detected activations extending over the motor, premotor and supplementary motor areas, but not in the prefrontal cortex. Thus, we finally focused on the prefrontal cortex and examined its activation during apple peeling in 12 subjects using a multichannel NIRS. We subsequently found that regional concentrations of oxygenated hemoglobin significantly increased in the measured region, which encompassed portions of the dorsolateral, ventrolateral and frontopolar areas of the prefrontal cortex. The current study demonstrated that apple peeling as practiced in daily life recruited the prefrontal cortex but that such activation might not be detected for less laborious mock apple peeling that can be performed in an fMRI environment. We suggest the importance of cortical study of an everyday task as it is but not as a simplified form; we also suggest the validity of NIRS for this purpose. Studies on everyday tasks may serve as stepping stone toward understanding human activities in terms of cortical activations.

Keywords: Near-infrared spectroscopy; NIRS; Prefrontal cortex; Simultaneous measurement; fMRI; Apple peeling; Everyday tasks

Introduction

It is intriguing to explore human brain activities during various daily operations. Cortical activity during daily operations may be deduced from fundamental mechanisms of human brain functions, but an a priori prediction does not always guarantee an accurate conclusion. Thus, to find cortical activity of a given everyday task, it is best to measure it directly.

Most everyday tasks are difficult to perform in restricted conditions of conventional functional imaging techniques, such as functional magnetic resonance imaging (fMRI) and positron emission tomography (PET). The most promising alternative, noninvasive neuroimaging method, may be near-infrared spectroscopy (NIRS) (reviewed in Villringer and Chance, 1997). NIRS monitors regional relative changes of hemoglobin concentration to measure cortical activation, utilizing the tight coupling between neural activity and regional cerebral blood flow (Villringer and Dirnafl, 1995). NIRS requires only compact experimental systems and is less restrictive (Fig. 1A), allowing subjects to engage in many daily human activities during measurement. Moreover, NIRS is more robust to body motion than other neuroimaging modalities and has proven to be effective in evaluating motor functions (Colier et al., 1999; Hirth et al., 1996; Maki et al., 1995; Obrig et al., 1996; Watanabe et al., 1996). In the most extreme conditions, NIRS was able to measure cortical activity of subjects walking on a treadmill (Miyai et al., 2001). The recent advent of a multichannel version of NIRS has expanded its technical potential for human brain mapping (Hoshi et al., 2000; Isobe et al., 2001; Miyai et al., 2001; Noguchi et al., 2002; Takahashi et al., 2000; Watanabe et al., 1996).

Thus, using the multichannel NIRS, we examined cortical activity during apple peeling with a knife as an example of an everyday task. We basically adopted a multimodal approach. fMRI enables whole-brain functional scanning but possesses poor task flexibility for the study of everyday tasks. In contrast, NIRS analysis is confined to only a small region of interest in the lateral cortical surface (Hoshi et al., 2000; Isobe et al., 2001; Miyai et al., 2001; Noguchi et al., 2002; Takahashi et al., 2000; Watanabe et al., 1996) but allows more flexible task selection than fMRI (Miyai et al., 2001). Since the two neuroimaging techniques are rather complementary, their combination should provide different perspectives on the study of everyday tasks.

* Corresponding author. National Food Research Institute, 2-1-12 Kannondai, Tsukuba, Ibaraki 305-8642, Japan. Fax: +81-298-38-8122.
E-mail address: dan@nfri.affrc.go.jp (I. Dan).
[1] Both authors contributed equally to this work.
Available online on ScienceDirect (www.sciencedirect.com.)

1053-8119/$ - see front matter © 2004 Elsevier Inc. All rights reserved.
doi:10.1016/j.neuroimage.2003.12.003

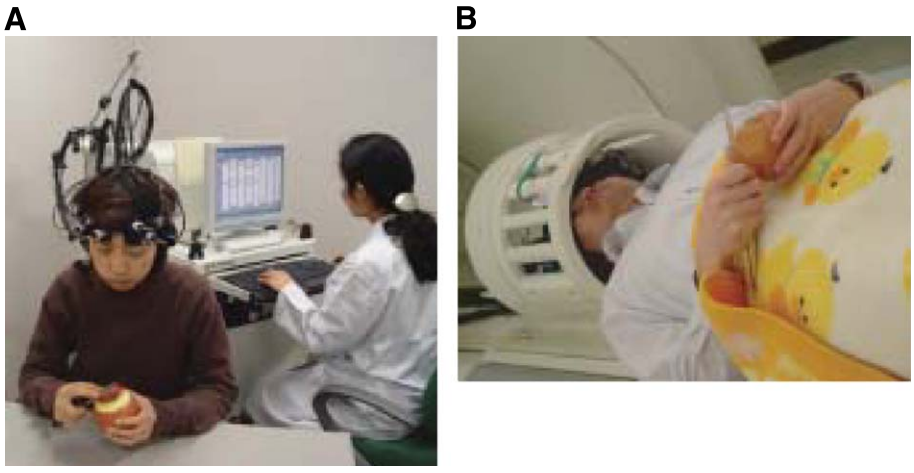

Fig. 1. Experimental conditions. (A) Instrument setting of NIRS, and a subject peeling an apple with a cooking knife. Six NIRS detector–illuminator pairs placed on the subject's forehead using a holder made of thermoplastic resin are connected to the main controlling unit via optic cables. (B) Experimental environment for simultaneous measurement using NIRS and fMRI. A subject, lying supine in an fMRI environment, performs a mock-peeling task while observing his hands, an apple and a plastic knife model through a mirror.

Several groups have succeeded in simultaneous measurements using fMRI and NIRS (Benaron et al., 2000; Cannestra et al., 2001; Kleinschmidt et al., 1996; Toronov et al., 2001a,b) including quantitative comparison between fMRI and NIRS signals (Strangman et al., 2002), but more applied study has yet to be performed.

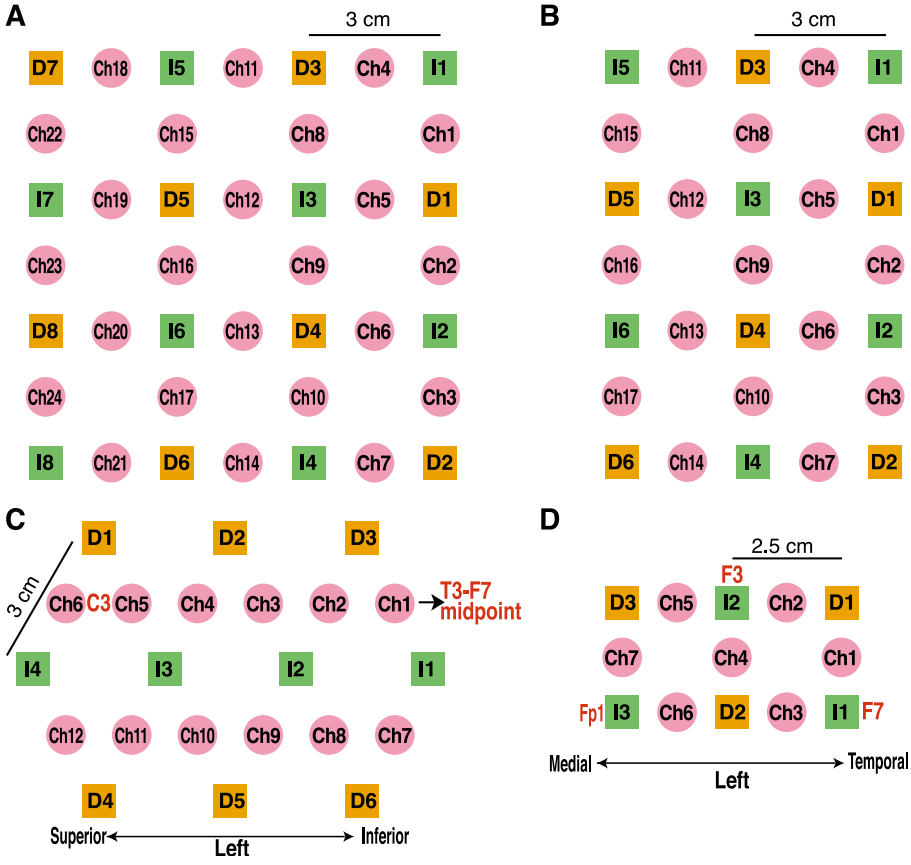

Fig. 2. NIRS channel setting. Illuminators are represented by green squares; detectors, by orange squares; and NIRS channels, by circles. (A) 24 NIRS channels for midline placements. (B) 17 × 2 NIRS channels for bilateral placements. Only channels in the left hemisphere are shown. (C) 12 × 2 NIRS channels for the motor area study. The international 10–20 standard positions and other positional information are indicated. Only channels in the left hemisphere are shown. (D) 7 × 2 NIRS channels for the prefrontal study. The international 10–20 standard positions and other positional information are indicated. Only channels in the left hemisphere are shown.

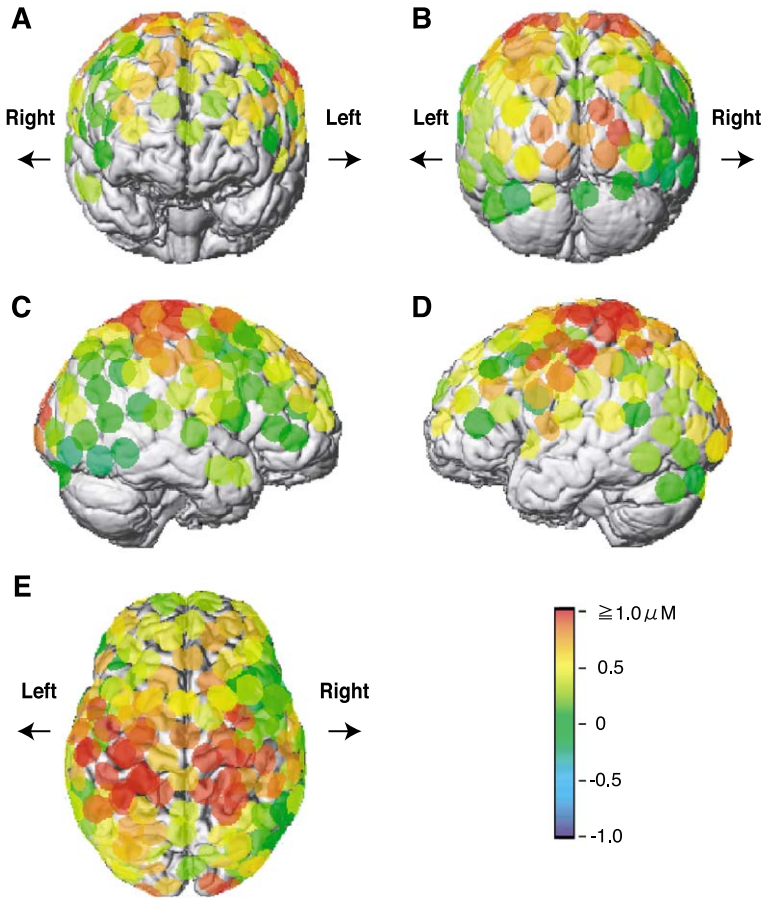

Fig. 3. Sequential whole-head examination by NIRS. Degree of activation in each NIRS channel during apple peeling task is shown as indicated in the color bar (Δ[oxyHb]). Directions are indicated when necessary. Average data for 10 replicated cycles (allowing for missing data) in a subject are overlaid on a normalized brain image of the subject. (A) Frontal view. (B) Occipital view. (C) Right temporal view. (D) Left view. (E) Top view.

Hence, we conducted five-step sequential multimodal studies to assess cortical activations during apple peeling as an example of an everyday task. First, we surveyed cortical activity during actual apple peeling by extensive sequential examination over the whole lateral cortical surface using multichannel NIRS in a pilot study. Second, we sought to establish a technical link between fMRI and NIRS analyses using simultaneous measurement of cortical activity during mock apple peeling by comparative signal correlation

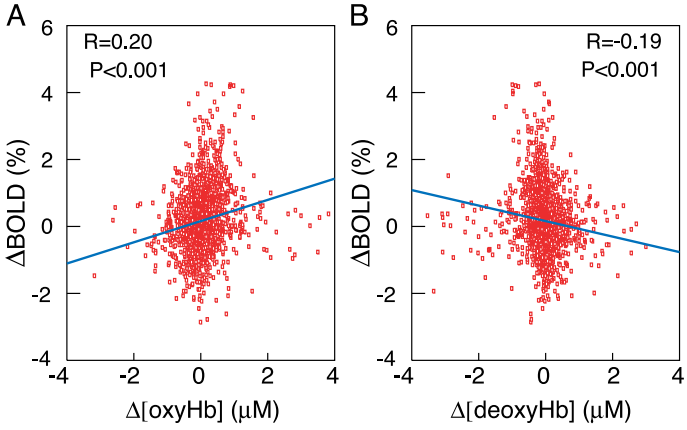

Fig. 4. Scatter plots of ΔBOLD versus Δ[oxyHb], and ΔBOLD versus Δ[deoxyHb] during mock-peeling task. Data points were collected from all the NIRS channels in the motor area of all the time series points of fMRI measurement (i.e., every 5 s). A regression line for the data points is drawn in blue. Spearman correlation functions were indicated by *R*. Probabilistic values against correlation with $R = 0$ were indicated by *P*. (A) ΔBOLD versus Δ[oxyHb]. (B) ΔBOLD versus Δ[deoxyHb].

analysis focusing on the motor area. Third, we focused on the prefrontal cortex and examined whether it is activated during the mock-peeling task by simultaneous measurement. Fourth, we examined the difference between fMRI and ordinary environments and made a link between the simultaneous and stand-alone NIRS measurements. As these experiments suggested prefrontal activation during apple peeling, we subsequently verified such activation using multichannel NIRS for a larger subject group. With this multimodal approach, we cultivated the possibility of examining everyday tasks as a novel application of neuroimaging techniques.

Methods

Subjects

The subjects in the whole-head examination by NIRS were two healthy volunteers (33-year-old male and 25-year-old female). The subjects in the simultaneous measurement by fMRI and NIRS were four healthy volunteers (three males and one female, aged 24–52 years). Twelve healthy volunteers participated in the prefrontal study (five males and seven females, aged 23–52 years). All were

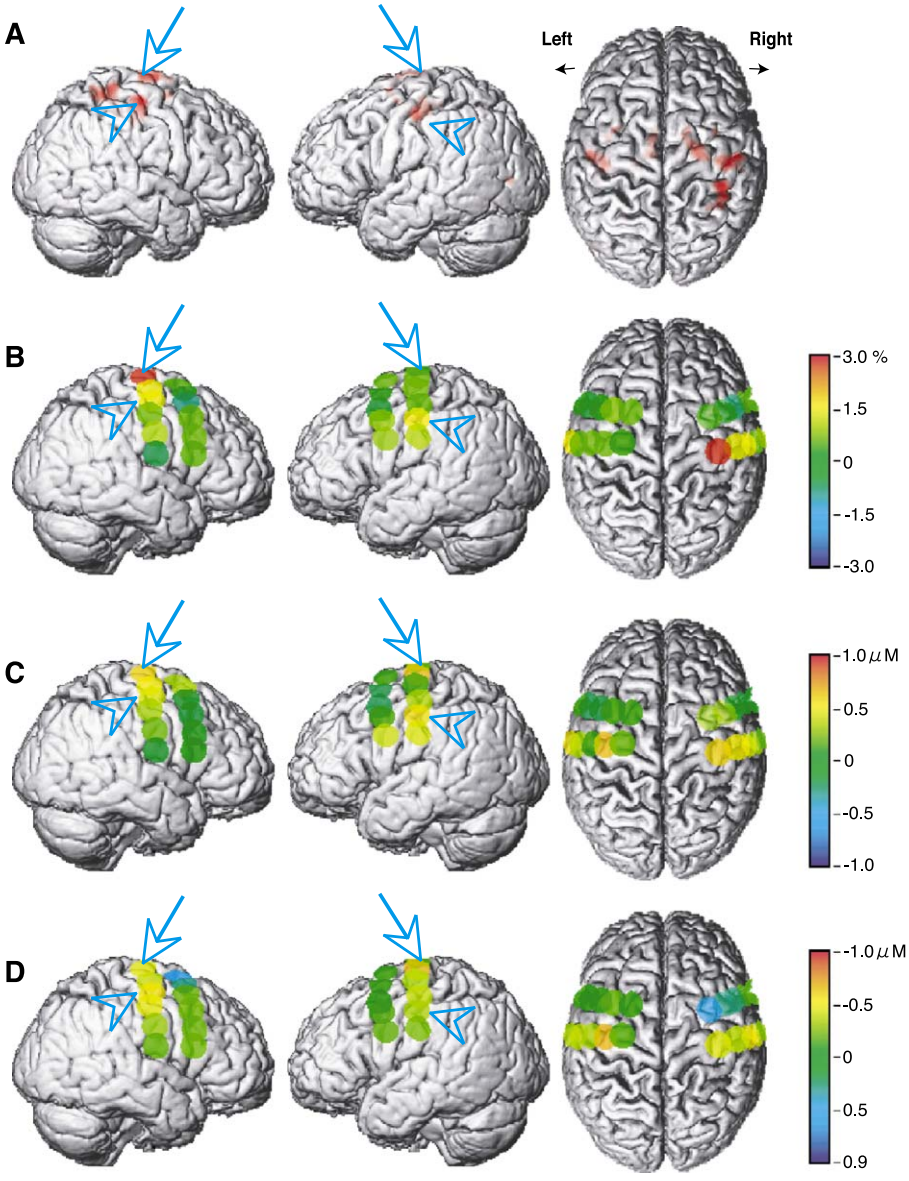

Fig. 5. Simultaneous measurement targeting the motor area. The left column presents right temporal views; middle column, left temporal views; and right column, top views. (A) SPM analysis of fMRI data. Activated voxels in fMRI data are shown in red (activation, $P < 0.05$, corrected). Arrows indicate the activation foci around the primary motor cortices and arrowheads indicate those in the sensory cortices in both hemispheres. These arrows and arrowheads are inserted at the same positions on the MR images in B, C and D to indicate the activation foci detected by the SPM analysis. (B) ΔBOLD analysis of fMRI data. ΔBOLD in the regions corresponding to putative NIRS channels are shown as indicated in the color bar. (C) Δ[oxyHb] analysis of NIRS data. Δ[oxyHb] values in the NIRS channels are shown as indicated in the color bar. (D) Δ[deoxyHb] analysis of NIRS data. Δ[deoxyHb] values in the NIRS channels are shown as indicated in the color bar. Directions are indicated when necessary. Brain images of a subject normalized to the MNI152 are shown. Scales of the color bars were determined by normalizing the ΔBOLD, Δ[oxyHb] and Δ[deoxyHb] data to their standard deviations.

right-handed. Written informed consents and an approval from the institutional ethics committee were obtained.

Materials

Apples (*Malus domestica* cultivar Fuji) of similar size (approximately 8 cm in diameter) were purchased from a local market. An ordinary 30-cm-long cooking knife with a 16-cm-long blade was used for peeling. Since virtually all commercially available cooking knives are magnetic, we made a nonmagnetic, full-scale model of the cooking knife, using wood and polyvinyl chloride plastic for the fMRI experimental environment (Fig. 1B).

Experimental design

Two experimental paradigms, apple peeling and mock peeling, were used in this study. The apple-peeling and mock-peeling paradigms were block designs consisting of (1) resting, (2) task, and (3) post-task resting periods. Each phase lasted 20 s. The paradigm was replicated for 10 cycles. Subject behavior was

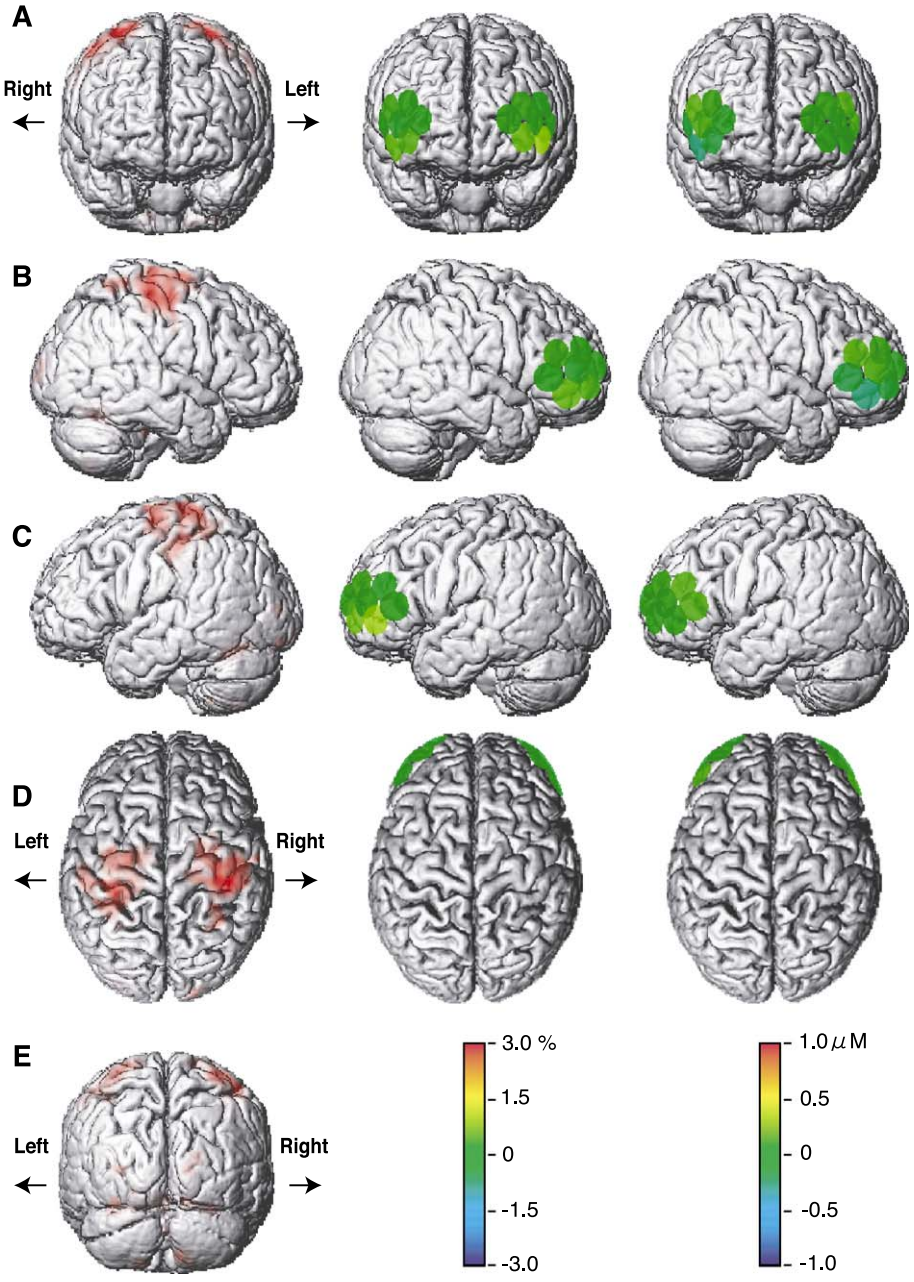

Fig. 6. Simultaneous measurement targeting the prefrontal area. In the left column, activated voxels in SPM analysis of fMRI data are shown in red (activation, $P < 0.05$, corrected). In the middle column, ΔBOLD in the regions corresponding to putative NIRS channels are shown as indicated in the color bar. In the right column, Δ[oxyHb] in the NIRS channels are shown as indicated in the color bar. Directions are indicated when necessary. Average data for 10 replicate cycles (allowing for missing data) in four subjects are overlaid on a normalized brain image of a subject. (A) Frontal view. (B) Right temporal view. (C) Left view. (D) Top view. (E) Occipital view (SPM analysis only).

monitored by an experimenter in stand-alone NIRS studies or by video recording in simultaneous measurements, and the cycles containing event-related noises such as coughing and sudden head movement were removed for later analysis.

In the apple-peeling task paradigm, subjects were requested to hold and turn an apple with their left hand while peeling it with a cooking knife held in their right hand during the task period, and to hold the apple with their left hand and the cooking knife with their right hand without moving them during the rest periods (Fig. 1A). We requested each subject to peel the apple at his/her own pace. The subjects performed the paradigms with their eyes open (spontaneous blinking was allowed).

In the mock-peeling task paradigm, subjects held an apple in their left hand and turned it while sliding a knife held in their right hand over its surface without actually peeling the apple. Before the current study, we observed that the mock-peeling task was performed slightly faster (4.1 ± 0.8 rotation/min, $N = 8$) than the apple-peeling task (3.3 ± 0.4 rotation/min, $N = 8$). Since the difference was approximately 20%, we requested the subjects to perform the mock-peeling task at approximately the same speed as they performed the apple-peeling task.

In the sequential whole-head examination by NIRS, subjects performed an apple-peeling task paradigm. During the experiment, the subjects sat on a chair in a relaxed position in a quiet room. We performed six separate measurements with different optode placements for each subject to cover the whole lateral cortical surface, since there were 12 illuminators and detectors in this study. The paradigm was replicated for 10 cycles for each measurement. We did not extend the whole-head examination for more than two subjects primarily because measurement of the optode locations in reference to the international 10–20 system for electrode placement (Jasper, 1958) took long and we could not avoid fatiguing the subjects.

In simultaneous measurements using fMRI and NIRS, subjects performed the mock-peeling task paradigm, since it was technically difficult to perform the apple-peeling task in an fMRI environment due to magnetism of cooking knives (Fig. 1B). The subjects performed the mock-peeling task in a supine position, monitoring their hand movement using a mirror.

In the NIRS-alone prefrontal studies, the subjects performed the apple-peeling and mock-peeling task paradigms in a sitting position as described above.

Placement of NIRS channels

NIRS channels were defined as the midpoint of corresponding detector–illuminator pairs. In the sequential whole-head examination, there were six optode placements (three midline and three bilateral placements) to cover the whole head for each subject. We used a thermoplastic holder embedded with eight illuminators and detectors, resulting in 24 channels for midline placements (Fig. 2A), and a pair of holders each embedded with six illuminators and

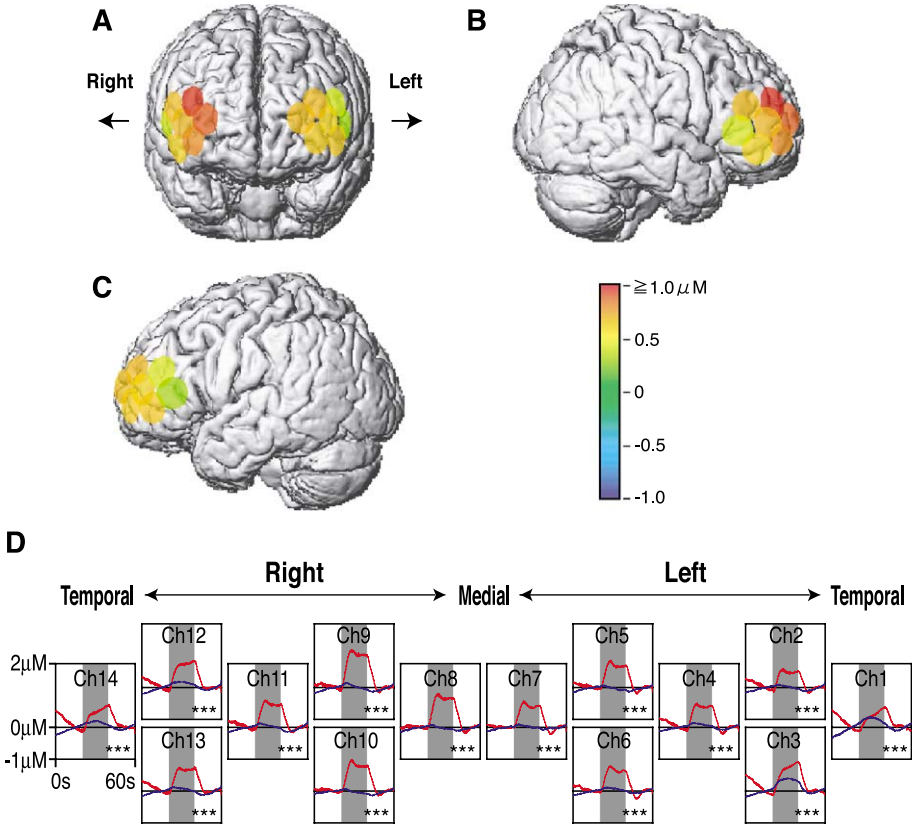

Fig. 7. Cortical activation during apple-peeling task detected by NIRS. An activation map assessed by NIRS is shown as indicated in the color bar (Δ[oxyHb]). Directions are indicated when necessary. Average data for all cycles in all subjects are overlaid on a normalized brain image of a subject. (A) Frontal view. (B) Right temporal view. (C) Left view. (D) Regional hemoglobin concentration changes during apple-peeling task. Δ[oxyHb] (red) and Δ[deoxyHb] (blue) are plotted versus time (s) for each NIRS channel. Task periods are highlighted with a gray background. Grand average data for 12 subjects and 10 replicated cycles (allowing for missing data) are shown. The channels exhibiting significant activation are indicated with asterisks.

detectors, resulting in 17 channels (34 in total) for bilateral placements (Fig. 2B). The inter-optode distance was set to 3 cm. Three midline and three bilateral placements generated 174 channels along the entire head. Locations of all channels on the subject's head surface were determined based on the international 10–20 system for electrode placement (Jasper, 1958).

In the simultaneous measurement by fMRI and NIRS, we used a pair of thermoplastic holders, each embedded with four illuminators and six detectors, resulting in 12 channels (24 in total) for the motor area study (Fig. 2C). The inter-optode distance was set to 3 cm. In the left hemisphere, the channels were placed so that the midpoint between channels 5 and 6 fit to C3 of the international 10–20 system and a line connecting channels 1 to 6 crossed at the midpoint of T3 and F7 (Fig. 2C). Channels in the right hemisphere were symmetrically set as well.

For the prefrontal study, we used a pair of holders, each embedded with three illuminators and detectors, resulting in seven channels for each holder (14 in total) (Fig. 2D). The inter-optode distance was set to 2.5 cm. The channels in the left hemisphere were placed so that the midpoint of channels 3 and 6 corresponded to the midpoint of Fp1 and F7. The channels were symmetrically placed in the right hemisphere as well. In the simultaneous measurement using fMRI and NIRS, we prepared all NIRS optodes and their holders using nonmagnetic materials. In the NIRS-alone prefrontal study, we used the same 14-channel optode settings as in the simultaneous fMRI and NIRS study (Fig. 2D).

NIRS measurement

We used an NIRS topography system, OMM-2000 Oxygenation Multichannel Monitor (Shimadzu, Kyoto, Japan), to monitor hemodynamic change (Fig. 1A). An illuminator fiber was connected to three laser diodes with wavelengths of 780, 805 and 830 nm. Each laser diode emitted 5-ms pulses of light. After 10 ms of lag time, light emission progressed from one light-source fiber to the next, preventing interference between light sources. After one sequential scan, we set an additional lag time of 10 ms. Illuminators that are separated more than 8 cm (e.g., I1 and I6 in Fig. 2A) are allowed to emit light simultaneously. Four sequential light emissions in the 24-channel NIRS resulted in $(5 + 10) \times 4 + 10 = 70$ ms in a scan. Similarly, scanning rates were 100 ms in the 17×2 channel NIRS, 70 ms in the 12×2 channel NIRS and 55 ms in the 7×2 channel NIRS. For each channel, five consecutive time points were accumulated to increase the signal-to-noise ratio, and their average was recorded. Thus, effective time resolutions became 500 ms in the 17×2 channel NIRS, 350 ms in the 12×2 and 24 channel NIRS, and 275 ms in the 7×2 channel NIRS. Irradiated light was detected at detector fibers connected to photomultiplier tubes sensitive to these wavelengths.

Optical data from individual illuminator–detector pairs were analyzed using the modified Beer–Lambert law (MBLL) for a highly scattering medium (Cope et al., 1988). According to the

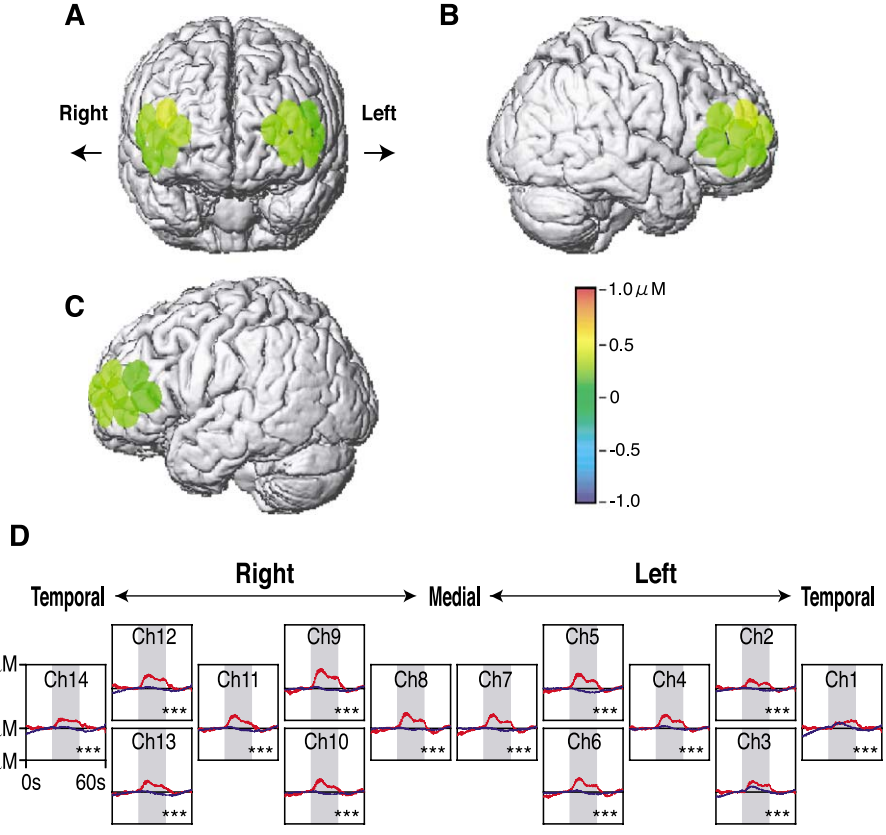

Fig. 8. Cortical activation during mock-peeling task detected by NIRS. An activation map assessed by NIRS is shown as indicated in the color bar (Δ[oxyHb]). Directions are indicated when necessary. Average data for all cycles in all subjects are overlaid on a normalized brain image of a subject. (A) Frontal view. (B) Right temporal view. (C) Left view. (D) Regional hemoglobin concentration changes during apple-peeling task. Δ[oxyHb] (red) and Δ[deoxyHb] (blue) are plotted versus time (s) for each NIRS channel. Task periods are highlighted with a gray background. Grand average data for 12 subjects and 10 replicated cycles (allowing for missing data) are shown. The channels exhibiting significant activation are indicated with asterisks.

MBLL, the change of absorbance at a given wavelength (ΔA_λ) can be represented as

$$\Delta A_\lambda = \varepsilon_\lambda \mathrm{DPF}\ L\ \Delta C \tag{1}$$

where ε_λ is the extinction coefficient at a given wavelength λ, DPF is the differential path length factor, L is the interoptode distance and ΔC is the change in concentration. Considering multiple measurements at three wavelengths, we rewrote Eq. (1) as

$$\begin{pmatrix} \Delta A_{780} \\ \Delta A_{805} \\ \Delta A_{830} \end{pmatrix} = \begin{pmatrix} \varepsilon_{780}^{\mathrm{HbO_2}} & \varepsilon_{780}^{\mathrm{HbR}} \\ \varepsilon_{805}^{\mathrm{HbO_2}} & \varepsilon_{805}^{\mathrm{HbR}} \\ \varepsilon_{830}^{\mathrm{HbO_2}} & \varepsilon_{830}^{\mathrm{HbR}} \end{pmatrix} \begin{pmatrix} \Delta[\mathrm{oxyHb}] \\ \Delta[\mathrm{deoxyHb}] \end{pmatrix} L\ \mathrm{DPF} \tag{2}$$

where Δ[oxyHb] and Δ[deoxyHb] are the changes in concentrations of oxygenated and deoxygenated hemoglobin. Using documented extinction coefficients (Matcher et al., 1995), we solved Eq. (2) by the least-squares method as

$$\begin{pmatrix} \Delta[\mathrm{oxyHb}] \\ \Delta[\mathrm{deoxyHb}] \end{pmatrix} = \frac{1}{L\ \mathrm{DPF}} \begin{pmatrix} -1.4887 & 0.5970 & 1.4847 \\ 1.8545 & -0.2394 & -1.0947 \end{pmatrix} \times \begin{pmatrix} \Delta A_{780} \\ \Delta A_{805} \\ \Delta A_{830} \end{pmatrix} \tag{3}$$

For each wavelength, the absorbance at the start of the rest period was selected as the initial absorbance. We assumed the DPF value was constant and set to 6 (van der Zee et al., 1992).

To remove signal drift from time series NIRS data, we set a linear base line with a slope. This was done primarily because the Hb parameters of NIRS and the blood oxygenation level dependent (BOLD) signal of fMRI often drifted in different directions for unknown reasons. We averaged Δ[oxyHb] and Δ[deoxyHb] from the 10th to the 20th second and from the 50th to the 60th second, and obtained Δ[oxyHb] and Δ[deoxyHb] for the two reference time points, i.e., 15th and 55th seconds. We then drew a baseline in the coordinate plane with a Δ[Hb] and time as each axis, crossing the Δ[Hb] values at the two reference points for both hemoglobin species. All Δ[Hb] data were normalized to the thus-determined baseline.

Statistical analysis of NIRS data

Δ[oxyHb] was evaluated statistically. We calculated the average Δ[oxyHb] during rest and task periods for each channel. Data obtained in the first 5 s were excluded to avoid transition period effects. For each paradigm, we calculated the average Δ[oxyHb] of a rest period by averaging the Δ[oxyHb] for the 5th to the 20th second, and that of a task period from the 25th to the 40th second. Values obtained in this way could not satisfy the criteria of equal variance, a statistical prerequisite for parametric tests, so we performed randomization tests (Edgington, 1995). For this purpose, we developed a computer program based on the MATLAB platform (The MathWorks, Inc.) (Dan et al., in press).

To compare activations during task and rest periods, we performed a three-way analysis of variance (ANOVA) randomization test, where the three ways consist of task or rest, subjects and cycles in each channel. The number of random permutation trials was set to 100,000, considering statistical validity for randomization test trials (Manly, 1997). We examined the differences in levels between task and rest. We performed 14 comparisons in the region of interest, so we multiplied P values (probability against a null hypothesis that there is no difference between effects) by a factor of 14 according to the Holm correction to reduce the type I error rate (Holm, 1979).

We compared degrees of activation among task kinds (e.g., between apple-peeling and mock-peeling tasks). For each task, we calculated the degree of activation by subtracting the average Δ[oxyHb] during the rest period (5th to the 20th second) from that during the task period (25th to the 40th second) in each cycle. We then performed repeated two-way ANOVA randomization tests for repeated measurement, where the two ways consisted of task kind (i.e., apple peeling or mock apple peeling) and subject, with each cell including corresponding cycles of data. We examined the differences in the levels between task kinds. The number of random permutation trials was set to 100,000. The obtained P value was corrected for multiple comparisons, as described above.

fMRI data collection and preprocessing

For simultaneous studies using fMRI and NIRS, we acquired functional and structural MRIs using a 1.5 T scanner (MAGNEX Eclipse PD250, Shimadzu) at the ATR Brain Activity Imaging Center (Kyoto, Japan). For functional imaging, we acquired T2*-weighted images using a gradient echo-planar imaging sequence (echo time 49 ms; repetition time 5000 ms; flip angle 90°). A total of 50 contiguous axial slices covering the cerebral cortex and cerebellum was acquired with a 3 × 3 × 3 mm voxel resolution. Anatomical T1-weighted MRI scans were also acquired for each individual with a 1 × 1 × 1 mm voxel resolution.

The MR images were preprocessed using the SPM99 program. The images were first motion-corrected and then spatially normalized (2 × 2 × 2 mm) to a standard Montreal Neurological Institute (MNI) 152 template. They were smoothed using an 8-mm FWHM Gaussian kernel. Regional brain activity changes between task and rest periods were assessed voxel by voxel using the SPM99 program. We adopted a fixed-effect model for both single subject study and for group analysis. The data were modeled using a box-car function convolved with the hemodynamic response function. Global normalization, grand mean scaling and a high-pass filter (minimum cutoff period of 120 s) were used. A statistical threshold was set at $P < 0.05$ (corrected for multiple comparisons).

Registration of NIRS channels onto MR images

In sequential whole-head examination, locations of all channels on the subjects' structural images were determined based on the international 10–20 standard positions. Since correspondence between the 10–20 positions and their underlying cortical structures had been fully examined for the subjects, we registered the NIRS channels on a structural MR image of each subject by interpolation, based on the international 10–20 standard positions using the MRIcro program (Rorden and Brett, 2000).

In the simultaneous measurement using fMRI and NIRS, we placed fatty pine nut markers on the NIRS optode holders, and identified the location of NIRS optodes and channels in the MR coordinate space via guidance of these markers. To project the identified positions on the head surface to the cortical surface of a structural MR image, we followed the method in our previous study (Okamoto et al., 2004). Basically, we defined the cortical projection point of an optode or channel as the closest point on the cortical surface to its position on the head surface.

In the prefrontal study using NIRS, we referred to our previous study to register NIRS channels on structural MR images (Okamoto et al., 2004). Briefly, fatty positional markers made of pine nuts were placed on the head surface according to the international 10–20 system. MR images were acquired using a 1.0-T MR scanner (MAGNEX EPIOS10, Shimadzu). A T1-weighted, three-dimensional gradient-echo sequence was used to produce 256 continuous axial 1-mm slices covering the entire cerebrum and head-surface markers (repetition time 37 ms; echo time 10 ms; flip angle 30°). The brain images were extracted from the T1 images that had been normalized to the MNI152 template using the SPM99 program (Friston et al., 1995). Meanwhile, the 10–20 markers on the head surface were projected onto the cortical surface. These positions were also normalized to the MNI152 template, and thus we obtained their probabilistic distributions among subjects in the MNI space. The standard deviation from the average 10–20 cortical projection to those in the subjects was 4–7 mm in the MNI space among the prefrontal regions examined. We anatomically labeled the cortical projections of the 10–20 standard positions in each subject and determined their probabilistic distributions. The anatomical correspondence between the 10–20 positions and underlying cortical structures was fairly good in the prefrontal regions. We estimated the most likely anatomical locations of the 14 prefrontal channels according to Talairach and Tournoux (1988) as shown in Table 1. We registered NIRS channels onto an MR image of a subject that was normalized to the MNI152 template as described above.

For presentation of hemodynamic data of NIRS and BOLD signal data of fMRI on 3D MR images, we first drew a sphere with a radius of 1 cm centering on the location of the registered channel using a computer program previously described (Okamoto et al., 2004). We then overlaid the sphere with a 3D MR image using the MRIcro program (Rorden and Brett, 2000) and determined the cross section of the sphere and brain surface. Finally, we painted the cross section with a color showing the degree of activation.

Table 1
Estimated anatomical locations of NIRS channels in the prefrontal study

Channel	Gyrus	Broadmann area
1, left 14, right	The triangular part of the inferior frontal gyrus	BA45
2, left 12, right	The middle frontal gyrus	BA46
3, left 13, right	The orbital part of the inferior frontal gyrus	BA46–47 border
4, left 11, right	The middle frontal gyrus	BA46–10 border
5, left 9, right	The border region of the superior and middle frontal gyri	BA9–10–46 border
6, left 10, right	The anterior region of the middle frontal gyrus	BA10
7, left 8, right	The border region of the superior and middle frontal gyri	BA10

Quantitative comparison of NIRS and BOLD signals

To compare NIRS and MR signals, we extracted the BOLD signal from voxels localized to the regions where each NIRS channel (midpoint of illuminator–detector pair) was set. To set regions of interest (ROI) corresponding to the NIRS channels, we first projected NIRS optodes and channels onto the cortical surface and identified their coordinates in T1-weighted structural MR space as described in the previous section. We then coregistered structural MR images to T2*-weighted MR images, and normalized them to the MNI152 template using the program SPM99. The identified positions of NIRS channels and optodes on the cortical surface of a structural MR image were also coregistered and normalized using the same parameters. We thus obtained their coordinates in the normalized MNI space. We then drew ROI as a sphere with a radius of 1 cm centering on the NIRS channel and extracted raw BOLD signal time series from fMR images as an average over the voxels localized in each ROI. Additionally, we drew ROI as a cylindrical shape, by first drawing two spheres with radii of 1 cm centering on the cortically projected points of optodes and then horizontally connecting the spheres. To build up ROI and extracting signals, we used MRIcro program (Rorden and Brett, 2000) and the MarsBaR toolbox for SPM99 (Brett et al., 2002). The extracted BOLD signal was corrected for signal drift using the same method as applied to NIRS data, and the change in BOLD signal (ΔBOLD) was calculated as a value relative to that of the baseline at each time series point.

We used signals obtained from simultaneous measurement by NIRS and fMRI targeting the motor area for quantitative comparison of NIRS and MR time series. To quantify the correspondence between NIRS and fMRI signals, 5-s intervals of the NIRS time series were averaged to reduce the oxyHb and deoxyHb signals to the BOLD signal time base. These data were collected for all channels, and ΔBOLD was then correlated with the computed Δ[oxyHb] and Δ[deoxyHb]. Scatterplots of resulting ΔBOLD vs. Δ[oxyHb] and vs. Δ[deoxyHb], and the corresponding Spearman correlation coefficients (R) were obtained.

To depict the degree of task-related activation for NIRS data, we subtracted an average of Δ[oxyHb] during the rest period (5th to the 20th second) from that during the task period (25th to the 40th second) and averaged the obtained value across all replicated cycles and subjects. For comparison, we also calculated ΔBOLD in the same region as the NIRS study. We subtracted the average of ΔBOLD during the rest period (5th to the 20th second) from that during the task period (25th to the 50th second) and averaged the obtained value across all replicated cycles and subjects. The activation data thus obtained were presented on 3D MR images as described above.

Results

Whole-head NIRS sequential examination during apple peeling

To find a global cortical activation pattern during actual apple peeling, we first performed a pilot study where we sequentially examined the whole lateral cortical surface by NIRS. Fig. 3

presents the results of a whole-head NIRS examination study showing the regional Δ[oxyHb] in 172 channels along the lateral cortices of one subject during an apple-peeling task. As expected for a task requiring elaborated motor coordination, channels exhibiting activations with over 1.0 μM Δ[oxyHb] increase are distributed on the primary motor, premotor, supplementary motor and anterior parietal areas. Activations in visual and sensory cortices were also detected. Moreover, prefrontal channels also exhibited relatively high activation with about 0.5 μM Δ[oxyHb] increase. Whole-head examination on the other subject resulted in a similar cortical activation pattern (data not shown).

However, the sequential whole-head examination put too much burden on subjects, and we could not extend the pilot study to a larger subject group. Therefore, we decided to assess the cortical activation pattern by fMRI using a more simplified task, to establish a technical link between fMRI and NIRS. We then examined cortical activity during apple peeling by NIRS, focusing on the prefrontal cortex.

Signal comparison by simultaneous fMRI and NIRS measurements targeting motor area

To establish a technical link for the comparative fMRI and NIRS study, we sought appropriate methods to compare signals of the two modalities and examined the correlation between the ΔBOLD detected by fMRI, and Δ[oxyHb] and Δ[deoxyHb] measured by NIRS. Thus, we performed simultaneous measurement using fMRI and NIRS that targeted on the motor area. Since actual apple peeling could not be performed in an fMRI environment because of metallic interference, we examined cortical activities during the mock-peeling task.

Fig. 4 depicts scatter plots of ΔBOLD vs. Δ[oxyHb] and ΔBOLD vs. Δ[deoxyHb]. There was a small but significant positive correlation between ΔBOLD and Δ[oxyHb] ($R = 0.20$, $P < 0.001$). Also, a similar level of significant negative correlation was found between the ΔBOLD and the Δ[oxyHb] concentration ($R = -0.19$, $P < 0.001$). The small correlation could be due to noise in Δ[oxyHb] and Δ[deoxyHb] measured by NIRS, since data accumulation of 10 cycles that could reduce noise level resulted in higher correlations ($R = 0.35$, $P < 0.001$ for Δ[oxyHb] and $R = -0.36$, $P < 0.001$ for Δ[deoxyHb]).

The BOLD signal was extracted either as a sphere centering on the midpoint of optode locations or as a cylindrical shape to better mimic the optical path of near-infrared light. Since the cylindrical methods resulted in similar levels of correlations ($R = 0.24$, $P < 0.001$ for Δ[oxyHb] and $R = -0.22$, $P < 0.001$ for Δ[deoxyHb], without data accumulation), we extracted ΔBOLD from a region defined by a sphere for the rest of the study.

Fig. 5 depicts the cortical activation pattern during the mock-peeling task as examined by four different methods, SPM and ΔBOLD analyses for fMRI data, and Δ[oxyHb] and Δ[deoxyHb] analyses for NIRS data. Activation patterns expressed as Δ[oxyHb] of NIRS and ΔBOLD of fMRI were fairly consistent. The SPM method detected four activation foci, the primary motor cortices (arrows) and the sensory cortices (arrowheads) in both hemispheres in the region examined by the other three methods. The ΔBOLD and Δ[oxyHb] methods yielded similar activation patterns except that the former failed to detect the activation focus on the primary motor cortex in the left hemisphere. The activation foci on the motor cortex in the left hemisphere and the sensory cortex in the right hemisphere were also detected by the Δ[deoxyHb] method, but the other two activation foci were not clear.

Simultaneous fMRI and NIRS measurement on the prefrontal cortex during mock-peeling task

We selected the prefrontal region as the target for NIRS analysis to see whether a mock-peeling task evokes task-related activation in this region. Fig. 6 displays the results of simultaneous measurements for four subjects. SPM analyses consistently detected significant cortical activation in motor, premotor and supplementary motor cortices. Also, activation was detected in the visual and sensory cortices. In contrast, fMRI did not detect significant activation in the prefrontal cortex of any of the subjects by SPM analyses, and there was a little increase (less than 0.8%) in ΔBOLD. Similarly, NIRS detected only a little (less than 0.1 μM Δ[oxyHb] increase) or no activation in the prefrontal region. When Δ[oxyHb] values between task and rest periods were statistically tested, no channel exhibited significant activation ($P < 0.05$, corrected for multiple comparisons).

Experimental link between fMRI and ordinary environments

Since it was technically difficult to perform a more realistic apple-peeling task in an fMRI environment, we examined cortical activation during actual apple peeling by stand-alone NIRS studies using the same subject group. We first examined if a mock-peeling task performed in a sitting position in an ordinary environment with a metal cooking knife can be regarded as comparable to that performed in a supine position in a fMRI environment with a plastic cooking knife using the same subject group. The mock-peeling task performed in an ordinary environment resulted in less than 0.2 μM Δ[oxyHb] increase. Statistical analysis detected a significant Δ[oxyHb] increase in channel 1 at $P < 0.05$ (data not shown). However, when the degree of activation during the task period was compared between the mock-peeling tasks performed in the fMRI and ordinary environments, there was no significant difference ($P < 0.05$, corrected).

Next, we examined the prefrontal activation during the apple-peeling task using the same subject group. All the channels examined exhibited Δ[oxyHb] increase of 0.2–0.7 μM, and the increases were statistically significant at $P < 0.01$ (data not shown). When the degree of activation during the task period was compared between the two tasks performed in an ordinary environment, there were significantly higher Δ[oxyHb] increases for the apple-peeling task in most dorsal channels (2, 4, 5, 6, 7, 8, 9 and 10; $P < 0.05$, corrected).

NIRS examination of prefrontal activity during apple peeling

Since the results presented above suggested involvement of the prefrontal cortex in apple peeling, we extended the NIRS prefrontal examination for larger subject group ($N = 12$). The region of interest was set to the prefrontal region extending over portions of the dorsolateral, ventrolateral and frontopolar areas. As shown in Fig. 7, we detected substantial cortical activation in all the channels examined. Some temporal channels, presumably located on and near the triangular part of the inferior frontal gyri, tended to exhibit smaller Δ[oxyHb] increases. At the beginning of the task period, Δ[oxyHb] started to increase and remained high until the end of the task period. At the beginning of the

post-task resting period, Δ[oxyHb] started to decrease to the basal level. However, the decline was overshot in some channels, so its effect extended beyond the rest period and into the next cycle. Δ[deoxyHb] changed little during the task period. In all the channels, the increase of Δ[oxyHb] during the apple-peeling task compared to that during the rest period was statistically significant at $P < 0.001$. We also examined the trial-dependent change of the prefrontal activations but we did not find any significant trial-dependent decrease of prefrontal activations (data not shown).

Moreover, we examined whether such activation could also be evoked by a less laborious, mock-peeling task for this subject group. During the mock-peeling task, we detected only lower-degree activation in all the channels (Fig. 8). Δ[oxyHb] during the mock-peeling task was significantly higher than that during the rest period at $P < 0.001$ in all channels. This higher statistical significance could be attributed to the increase of statistical validity achieved by using a larger subject group.

Comparing activation levels between the apple-peeling and mock-peeling tasks, Δ[oxyHb] was 0.2–0.6 μM greater in the apple-peeling task throughout the channels. Statistically comparing Δ[oxyHb] between the apple-peeling and control tasks revealed that Δ[oxyHb] was significantly higher in all 14 channels ($P < 0.01$, corrected).

Discussion

In the present study, we explored the possibility of applying neuroimaging techniques to study cortical activities during daily tasks of human beings. As a first step toward this goal, we examined cortical activations associated with apple peeling with emphasis on the prefrontal cortex using multichannel NIRS and fMRI. We begin this discussion by examining the technical validity of our approach with emphasis on technical bridge between the two imaging modalities. Next, we consider the functional compatibility of the present study with the known functions. Finally, we suggest the role of everyday tasks as guideposts for understanding various human activities in terms of cortical activations that underlie them.

Technical considerations for simultaneous measurement

There have been several simultaneous measurements using fMRI and NIRS (Benaron et al., 2000; Cannestra et al., 2001; Kleinschmidt et al., 1996; Strangman et al., 2002; Toronov et al., 2001a,b). However, methods to compare data obtained from the two modalities are yet to be established. First, selection of the hemoglobin species to represent NIRS cortical activation data is still an issue to be discussed. Currently, the most elaborate quantitative comparison by Strangman et al. (2002) revealed a higher correlation between ΔBOLD and Δ[oxyHb] and suggested this is due to a higher signal-to-noise ratio of the oxyHb than deoxyHb parameter. A NIRS signal study using a perfused rat brain model proposed that Δ[oxyHb] is the more sensitive parameter for activation study (Hoshi et al., 2001). Our simultaneous study detected similar levels of correlation for both hemoglobin parameters and could not provide a decisive conclusion on this issue. However, given the similar degree of correlation and higher signal-to-noise ratio of the oxyHb parameter, it is appropriate to represent NIRS data by Δ[oxyHb] for comparative study with fMRI. This view was supported by a comparison of activation patterns in four methods presented in the current study showing a slightly deviated pattern in the Δ[deoxyHb] method. We should add here that this selection is only valid when the time resolution is on the order of seconds and thus the early response, or localized deoxygenation in the early phase of functional activation, is negligible (Duong et al., 2000).

The next issue to be discussed is a data presentation method for comparative study. Activation data of fMRI studies are generally presented as probabilistic values rather than as ΔBOLD, and thus are not suitable for comparison with Δ[oxyHb] of NIRS. To present data from the two different modalities in comparable forms, we used the spherical extraction method to extract the BOLD signal from the voxels localized to the regions where each NIRS channel (midpoint of an illuminator–detector pair) was set. We also attempted the cylindrical extraction method to better mimic the optical path. This resulted in slightly better correlation, but also turned out to be too laborious for routine analysis. A BOLD signal extraction method based on a simulation (Okada et al., 1997) might better represent the actual optical path and thus might realize a better correlation.

As shown in Fig. 4, ΔBOLD of fMRI and Δ[oxyHb] of NIRS were positively correlated. A better correlation was obtained when data of all the cycles were accumulated and averaged, probably due to noise reduction. Therefore, comparison of the two parameters should be fairly valid on a semiquantitative level for simultaneous measurement. The SPM method was also consistent with Δ[oxyHb] of NIRS, but the comparison is valid only on the qualitative level since the two methods are based on different technical premises.

We expressed the Δ[oxyHb] data of NIRS and the ΔBOLD data of fMRI in the same manner on the cortical surface and used a topographic presentation to facilitate an intuitive grasp of the activation patterns. However, we should mention that such topographic presentation is valid only to a limited degree. First, since the cortical contribution to optical path length differs among channels, the spatial activation pattern might not be represented quantitatively among different channels (Boas et al., 2001). The topographic presentation of NIRS data in the current study was based on a modified Beer–Lambert law (Cope et al., 1988) with an equal DPF assumption. For a more quantitative spatial analysis, more elaborate examination for optical path length is necessary. Second, there are problems of anatomical variability associated with intersubject data integration. Our previous study revealed variability associated with NIRS channel registration to MR images and intersubject data integration. The variability from an ideal brain in the MNI space was estimated to be 5 mm in terms of the standard deviation of the reference point of the prefrontal NIRS measurement (i.e., Fp1–F7 or Fp2–F8 midpoints). This means that statistically 61% of the reference points fall within 5 mm of the reference points of the ideal brain in the MNI space (Okamoto et al., 2004). The estimations for the other peripheral channels were slightly inaccurate but on similar orders. Taken together, we suggest that a rough semiquantitative functional comparison with a spatial resolution of 1 cm or so should be valid for the method we used in the current study.

One possible concern for NIRS-alone prefrontal study is that the significant increase of Δ[oxyHb] in all channels during the apple-peeling task may be due to global signals, or due to the contribution of noncortical blood flow change. Although we cannot completely exclude this possibility from the current experimental conditions, activation patterns observed in the whole-head studies that correlated fairly well to known functional localizations

suggest that multichannel NIRS detected the Δ[oxyHb] increase associated with cortical activations.

Functional compatibility

As demonstrated, we found that the prefrontal area is recruited during the apple-peeling task. The activation was more apparent in the dorso-anterior channels that were estimated to be on superior and middle frontal gyri, but the ventral channels over the inferior frontal gyrus were also significantly active. Thus, it seems appropriate to consider that the measured region, which encompassed portions of the dorsolateral, ventrolateral and frontopolar areas of the prefrontal cortex, is involved in apple peeling. The similar but more automatic mock-peeling task evoked activations in motor-related areas including the supplementary motor, premotor, primary motor and somatosensory cortices, but a lower degree of prefrontal activation.

Complex, self-paced finger movements are known to recruit the supplementary motor and somatosensory cortices in addition to the premotor and primary motor cortices that are activated by simple finger movements (Rao et al., 1993; Roland et al., 1982). The cortical activation pattern associated with the mock-peeling task observed in our fMRI study is consistent with those observations considering the nature of the mock-peeling task involving coordinated movement of fingers, thumbs and palms of both hands executed at internally triggered paces.

In addition to the activations in the motor-related regions, apple peeling recruited considerable activations in the prefrontal cortex. The prefrontal activation associated with motor tasks is intensively studied in motor learning. Learning of a novel motor performance is known to activate prefrontal cortices (Jenkins et al., 1994; Jueptner et al., 1997), but the activation disappears as learning progresses and the task thus is performed automatically (Passingham, 1996). However, the apple-peeling task does not likely involve learning since all subjects had experience in peeling apples and there was no apparent trial-dependent decrease of prefrontal activations over replicated cycles. A longer period of practice may enable automatic apple peeling, but such an occasion rarely happens in ordinary daily life. It is more appropriate to consider apple peeling as execution of already learned motor sequences.

Jueptner et al. (1997) found activation of the left dorsolateral prefrontal cortex when subjects were requested to pay attention to what they were doing when performing prelearned motor sequences of key pressing. Stephan et al. (2002) detected bilateral (somewhat right-oriented) activation of the dorsolateral prefrontal cortex associated with attention to externally triggered finger movement. Considering the substantial care for knife handling, apple peeling should require attention to the ongoing action, and thus the prefrontal activation observed in the current study is compatible with these former observations.

Another factor that needs to be considered is working memory, or the cognitive system that allows individuals to maintain and manipulate information held temporarily in their minds (Baddeley, 1992). Functional imaging studies of motor working memory based on delayed-response tasks revealed that the dorsolateral prefrontal cortex was recruited for short-term sensory memory and motor preparation (D'Esposito et al., 2000). How much working memory the apple-peeling task involves is the question that needs to be addressed. Studies on eye and hand movements during everyday tasks such as tea preparation, hand washing and sandwich making revealed that most eye fixations were related to ongoing action while some were relevant only to future actions (Hayhoe et al., 2003; Land et al., 1999; Pelz and Canosa, 2001). These studies suggested the involvement of working memory to provide continuity of perceptual experience. Considering the ubiquitous aspect of the look-ahead eye-fixation associated with these everyday tasks, the apple-peeling task that requires as much dexterity as these tasks likely also requires some working memory for its execution.

The prefrontal activation associated with apple peeling might also be appreciated in terms of an executive control function. Executive control functions are the coordinated operation of various processes to accomplish a particular goal in a flexible manner, and the prefrontal cortex is considered as their anatomical substrate (reviewed in Royall et al., 2002). The concept of an executive control function is broad in that it overlaps other cognitive functions such as working memory and attention mentioned above. Lezak (1995) offered simple criteria to define executive frontal system capacities, which include modification of ongoing behavior in response to dynamic task requirements. Apple peeling is not a fully automatic movement but a goal-oriented adjustment based on visual and somatosensory feedback, and thus should include executive control functions.

Everyday tasks as relay points for understanding complex human behavior

As discussed above, the prefrontal activation associated with apple peeling is compatible with the current view of the prefrontal functions, but the everyday task that we used in this study has a composite nature and therefore is not suitable for elaborate functional dissections. Instead, our aim lies in describing a cortical presentation of a composite everyday task as it is.

Most human activities are composite, and the cortical presentation associated with them should reflect the complex nature of the activities. One approach to understanding human activities in terms of brain function may be dissection and reconstruction, namely, deducing brain functions of a given activity from basic mechanisms of the brain revealed by functional dissections. Another plausible approach may be to describe cortical presentation for a given task and use the description as an anchoring point to consider human brain functions in various human behaviors.

Even formal neuropsychological tests do not represent a single brain function but include multiple dimensions. For example, the Wisconsin Card Sorting Test (Grant and Berg, 1948) is associated with concept generation, inhibition, planning and working memory (Malloy and Richardson, 1994). Although functional imaging studies for the test did not fully dissect functional constituents of the test in detail, the studies presented a neuroanatomical basis for the test (Berman et al., 1995; Marenco et al., 1993). Similarly, neuroimaging study of everyday tasks as we presented in the current study might present a neuroanatomical relay point to understand complex human activities in daily living in terms of brain functions.

Cognitive examinations based on everyday tasks (also called natural tasks) have been started in oculomotor behavioral studies (Hayhoe et al., 2003; Land et al., 1999; Pelz and Canosa, 2001) but have not been applied to neuroimaging analyses. Compact experimental setting and high-resilience to body movement of NIRS enabled functional examination of cortical activity during everyday tasks and may extend the potential of neuroimaging applications.

Acknowledgments

We thank the subjects who participated in this experiment, and the ATR Brain Imaging Center for their aid in fMRI data acquisition. We also thank Mr. Shigeo Tanaka for construction of instruments. This work is supported by the Program for Promotion of Basic Research Activities for Innovative Bioscience (PROBRAIN) (K.K. and I.D), and the Industrial Technology Research Grant Program in 03A47022 from the New Energy and Industrial Technology Development Organization (NEDO) of Japan (I.D.).

References

Baddeley, A., 1992. Working memory. Science 255, 556–559.

Benaron, D.A., Hintz, S.R., Villringer, A., Boas, D., Kleinschmidt, A., Frahm, J., Hirth, C., Obrig, H., van Houten, J.C., Kermit, E.L., Cheong, W.F., Stevenson, D.K., 2000. Noninvasive functional imaging of human brain using light. J. Cereb. Blood Flow Metab. 20, 469–477.

Berman, K.F., Ostrem, J.L., Randolph, C., Gold, J., Goldberg, T.E., Coppola, R., Carson, R.E., Herscovitch, P., Weinberger, D.R., 1995. Physiological activation of a cortical network during performance of the Wisconsin card sorting test: a positron emission tomography study. Neuropsychologia 33, 1027–1046.

Boas, D.A., Gaudette, T., Strangman, G., Cheng, X., Marota, J.J., Mandeville, J.B., 2001. The accuracy of near infrared spectroscopy and imaging during focal changes in cerebral hemodynamics. NeuroImage 13, 76–90.

Brett, M., Anton, J.L., Valabregue, R., Poline, J.B., 2002. Region of interest analysis using an SPM toolbox. NeuroImage 16, 497 (abstract).

Cannestra, A.F., Pouratian, N., Bookheimer, S.Y., Martin, N.A., Beckerand, D.P., Toga, A.W., 2001. Temporal spatial differences observed by functional MRI and human intraoperative optical imaging. Cereb. Cortex 118, 773–782.

Colier, W.N., Quaresima, V., Oeseburg, B., Ferrari, M., 1999. Human motor-cortex oxygenation changes induced by cyclic coupled movements of hand and foot. Exp. Brain Res. 129, 457–461.

Cope, M., Delpy, D.T., Reynolds, E.O., Wray, S., Wyatt, J., van der Zee, P., 1988. Methods of quantitating cerebral near infrared spectroscopy data. Adv. Exp. Med. Biol. 222, 183–189.

Dan, H., Watanabe, H., Dan, I., Kohyama, K., 2003. Effects of textural changes in cooked apples on the human bite and instrumental tests. J. Texture Stud. (in press).

D'Esposito, M., Ballard, D., Zarahn, E., Aguirre, G.K., 2000. The role of prefrontal cortex in sensory memory and motor preparation: an event-related fMRI study. NeuroImage 11, 400–408.

Duong, T.Q., Kim, D.S., Ugurbil, K., Kim, S.G., 2000. Spatiotemporal dynamics of the BOLD fMRI signals: toward mapping submillimeter cortical columns using the early negative response. Magn. Reson. Med. 44, 231–242.

Edgington, E.S., 1995. Randomization Test. Third ed. Dekker, New York.

Friston, K.J., Ashburner, J., Frith, C.D., Poline, J.B., Heather, J.D., Frackowiak, R.S.J., 1995. Spatial registration and normalization of images. Hum. Brain Mapp. 2, 165–189.

Grant, D.A., Berg, E.A., 1948. A behavioral analysis of the degree of reinforcement and ease of shifting to new responses in a Weigl-type card sorting problem. J. Exp. Psychol. 38, 404–411.

Hayhoe, M.M., Shrivastava, A., Mruczek, R., Pelz, J.B., 2003. Visual memory and motor planning in a natural task. J. Vis. 3, 49–63.

Hirth, C., Obrig, H., Villringer, K., Thiel, A., Bernarding, J., Muhlnickel, W., Flor, H., Dirnagl, U., Villringer, A., 1996. Non-invasive functional mapping of the human motor cortex using near-infrared spectroscopy. NeuroReport 7, 1977–1981.

Holm, S.A., 1979. A simple sequentially rejective multiple test procedure. Scand. J. Statist. 6, 71–76.

Hoshi, Y., Oda, I., Wada, Y., Ito, Y., Yamashita, Y., Oda, M., Ohta, K., Yamada, Y., Tamura, M., 2000. Visuospatial imagery is a fruitful strategy for the digit span backward task: a study with near-infrared optical tomography. Brain. Res. Cogn. Brain. Res. 9, 339–342.

Hoshi, Y., Kobayashi, N., Tamura, M., 2001. Interpretation of near-infrared spectroscopy signals: a study with a newly developed perfused rat brain model. J. Appl. Physiol. 90, 1657–1662.

Isobe, K., Kusaka, T., Nagano, K., Okubo, K., Yasuda, S., Kondo, M., Itoh, S., Onishi, S., 2001. Functional imaging of the brain in sedated newborn infants using near infrared topography during passive knee movement. Neurosci. Lett. 299, 221–224.

Jasper, H.H., 1958. The ten–twenty electrode system of the International Federation. Electroenceph. Clin. Neurophysiol. 10, 367–380.

Jenkins, I.H., Brooks, D.J., Nixon, P.D., Frackowiak, R.S., Passingham, R.E., 1994. Motor sequence learning: a study with positron emission tomography. J. Neurosci. 14, 3775–3790.

Jueptner, M., Stephan, K.M., Frith, C.D., Brooks, D.J., Frackowiak, R.S., Passingham, R.E., 1997. Anatomy of motor learning: I. Frontal cortex and attention to action. J. Neurophysiol. 77, 1313–1324.

Kleinschmidt, A., Obrig, H., Requardt, M., Merboldt, K.D., Dirnagl, U., Villringer, A., Frahm, J., 1996. Simultaneous recording of cerebral blood oxygenation changes during human brain activation by magnetic resonance imaging and near-infrared spectroscopy. J. Cereb. Blood Flow Metab. 165, 817–826.

Land, M., Mennie, N., Rusted, J., 1999. The roles of vision and eye movements in the control of activities of daily living. Perception 28, 1311–1328.

Lezak, M.D., 1995. Neuropsychological Assessment. Third ed. Oxford Univ. Press, New York, pp. 602–649.

Maki, A., Yamashita, Y., Ito, Y., Watanabe, E., Mayanagi, Y., Koizumi, H., 1995. Spatial and temporal analysis of human motor activity using noninvasive NIR topography. Med. Phys. 22, 1997–2005.

Malloy, P.F., Richardson, E.D., 1994. Assessment of frontal lobe functions. J. Neuropsychiatry Clin. Neurosci. 6, 399–410.

Manly, B.F.J., 1997. Randomization, Bootstrap and Monte Carlo Methods in Biology. Second ed. Chapman & Hall, London.

Marenco, S., Coppola, R., Daniel, D.G., Zigun, J.R., Weinberger, D.R., 1993. Regional cerebral blood flow during the Wisconsin card sorting test in normal subjects studied by xenon-133 dynamic SPECT: comparison of absolute values, percent distribution values, and covariance analysis. Psychiatry Res. 50, 177–192.

Matcher, S.J., Elwell, C.E., Cooper, C.E., Cope, M., Delpy, D.T., 1995. Performance comparison of several published tissue near-infrared spectroscopy algorithms. Anal Biochem. 227, 54–68.

Miyai, I., Tanabe, H.C., Sase, I., Eda, H., Oda, I., Konishi, I., Tsunazawa, Y., Suzuki, T., Yanagida, T., Kubota, K., 2001. Cortical mapping of gait in humans: a near-infrared spectroscopic topography study. NeuroImage 14, 1186–1192.

Noguchi, Y., Takeuchi, T., Sakai, K.L., 2002. Lateralized activation in the inferior frontal cortex during syntactic processing: event-related optical topography study. Hum. Brain Mapp. 17, 89–99.

Obrig, H., Hirth, C., Junge-Hulsing, J.G., Doge, C., Wolf, T., Dirnagl, U., Villringer, A., 1996. Cerebral oxygenation changes in response to motor stimulation. J. Appl. Physiol. 81, 1174–1183.

Okada, E., Firbank, M., Schweiger, M., Arridge, S.R., Cope, M., Delpy, D.T., 1997. Theoretical and experimental investigation of near-infrared light propagation in a model of adult head. Appl. Opt. 36, 21–31.

Okamoto, M., Dan, H., Sakamoto, K., Takeo, K., Shimizu, K., Kohno, S., Oda, I., Isobe, S., Suzuki, T., Kohyama, K., Dan, I., 2004. Three-dimensional probabilistic anatomical cranio-cerebral correlation via the international 10–20 system oriented for transcranial functional brain mapping. NeuroImage 21, 99–111.

Passingham, R.E., 1996. Attention to action. Philos. Trans. R. Soc. London, Ser. B 351, 1473–1479.

Pelz, J.B., Canosa, R., 2001. Oculomotor behavior and perceptual strategies in complex tasks. Vis. Res. 41, 3587–3596.

Rao, S.M., Binder, J.R., Bandettini, P.A., Hammeke, T.A., Yetkin, F.Z., Jesmanowicz, A., Lisk, L.M., Morris, G.L., Mueller, W.M., Estkowski, L.D., Wong, E.C., Haughton, V.M., Hyde, J.S., 1993. Functional magnetic resonance imaging of complex human movements. Neurology 43, 2311–2318.

Roland, P.E., Meyer, E., Shibasaki, T., Yamamoto, Y.L., Thompson, C.J., 1982. Regional cerebral blood flow changes in cortex and basal ganglia during voluntary movements in normal human volunteers. J. Neurophysiol. 48, 467–480.

Rorden, C., Brett, M., 2000. Stereotaxic display of brain lesions. Behav. Neurol. 12, 191–200.

Royall, D.R., Lauterbach, E.C., Cummings, J.L., Reeve, A., Rummans, T.A., Kaufer, D.I., LaFrance Jr., W.C., Coffey, C.E., 2002. Executive control function: a review of its promise and challenges for clinical research. A report from the Committee on Research of the American Neuropsychiatric Association. J. Neuropsychiatry Clin. Neurosci. 14, 377–405.

Stephan, K.M., Thaut, M.H., Wunderlich, G., Schicks, W., Tian, B., Tellmann, L., Schmitz, T., Herzog, H., McIntosh, G.C., Seitz, R.J., Homberg, V., 2002. Conscious and subconscious sensorimotor synchronization-prefrontal cortex and the influence of awareness. NeuroImage 15, 345–352.

Strangman, G., Culver, J.P., Thompson, J.H., Boas, D.A., 2002. A quantitative comparison of simultaneous BOLD fMRI and NIRS recordings during functional brain activation. NeuroImage 17, 719–731.

Takahashi, K., Ogata, S., Atsumi, Y., Yamamoto, R., Shiotsuka, S., Maki, A., Yamashita, Y., Yamamoto, T., Koizumi, H., Hirasawa, H., Igawa, M., 2000. Activation of the visual cortex imaged by 24-channel near-infrared spectroscopy. J. Biomed. Opt. 5, 93–96.

Talairach, J., Tournoux, P., 1988. Co-planar Stereotaxic Atlas of the Human Brain. Thieme, New York.

Toronov, V., Webb, A., Choi, J.H., Wolf, M., Michalos, A., Gratton, E., Hueber, D., 2001a. Investigation of human brain hemodynamics by simultaneous near-infrared spectroscopy and functional magnetic resonance imaging. Med. Phys. 28, 521–527.

Toronov, V., Webb, A., Choi, J.H., Wolf, M., Safonova, L., Wolf, U., Gratton, E., 2001b. Study of local cerebral hemodynamics by frequency-domain near-infrared spectroscopy and correlation with simultaneously acquired functional magnetic resonance imaging. Opt. Express 9, 417–427.

van der Zee, P., Cope, M., Arridge, S.R., Essenpreis, M., Potter, L.A., Edwards, A.D., Wyatt, J.S., McCormick, D.C., Roth, S.C., Reynolds, E.O.R., Delpy, D.T., 1992. Experimentally measured optical pathlengths for the adult head, calf and forearm and the head of the newborn infant as a function of interoptode spacing. Adv. Exp. Med. Biol. 316, 143–153.

Villringer, A., Chance, B., 1997. Non-invasive optical spectroscopy and imaging of human brain function. Trends Neurosci. 20, 435–442.

Villringer, A., Dirnafl, U., 1995. Coupling of brain activity and cerebral blood flow: basis of functional neuroimaging. Cerebrovasc. Brain Metab. Rev. 7, 240–276.

Watanabe, E., Yamashita, Y., Maki, A., Ito, Y., Koizumi, H., 1996. Non-invasive functional mapping with multi-channel near infra-red spectroscopic topography in humans. Neurosci. Lett. 205, 41–44.